ELSEVIER

NeuroImage

www.elsevier.com/locate/ynimg
NeuroImage 35 (2007) 655–668

Parsing a sequence of brain activations at psychological times using fMRI

M. Sigman,[a,b,*] A. Jobert,[b] D. LeBihan,[b] and S. Dehaene[b]

[a]*Integrative Neuroscience Laboratory Physics Department, FCEyN, UBA, Buenos Aires, Argentina*
[b]*INSERM-CEA unit 562 "Cognitive Neuroimaging", Service Hospitalier Frédéric Joliot, Orsay, France*

Received 25 September 2005; revised 14 May 2006; accepted 23 May 2006
Available online 1 February 2007

Identifying the sequence of computations which constitute a cognitive task is a fundamental problem in neuroscience. Here we show, using functional magnetic resonance imaging (fMRI), that we can parse, at the time scale of about 100 ms, the different stages of brain activations which compose a complex sequential task. To identify timing information from the slow blood oxygen level-dependent (BOLD) signal response, we use a simple analytic method, based on periodic stimulation and an analysis of covariation of the spectral parameters (phase and power spectrum at the stimulation frequency) with the different experimental conditions. We implement this strategy in a sequential task, where the onset and duration of different stages are under experimental control. We are able to detect changes in onset latency and in the duration of the response, in an invariant fashion across different brain regions, and reconstruct the stream of activations consistent with five distinct stages of processing of the task. Sensory and motor clusters activate in the expected order and for the expected duration. The timing of sensory activations is more precise than the timing of motor activation. We also parse in time the reading-verbal network: visual extrastriate and phonological access regions (supramarginal gyrus) activate at the time of word presentation, while the inferior frontal gyrus, the anterior cingulate and the supplementary motor area are activated during the rehearsal period.

Keywords: fMRI; Timing; Cognitive; Additive factors; Sequences; Language

Introduction

Mental chronometry seeks to measure the time course of mental operations in the nervous system. (Posner, 1978; Sternberg, 1969). A recent challenge has been to integrate psychological chronometric methods and imaging techniques, to observe the sequence of brain activations of a complex cognitive task. A series of previous studies have shown that fine temporal fMRI measurements (~100 ms) while not necessarily easy to achieve, are feasible (Buckner et al., 1996; Dale et al., 2000; Formisano et al., 2002; Henson et al., 2002; Kim et al., 1997; Lange and Zeger, 1997; Lee et al., 2005; Liao et al., 2002; Menon et al., 1998; Purdon et al., 2001; Richter et al., 1997a,b, 2000; Saad et al., 2003; Schacter et al., 1997; Thierry et al., 1999; Weilke et al., 2001; Wildgruber et al., 1999 for reviews, see Buckner, 2003; Formisano and Goebel, 2003; Menon and Kim, 1999; Rosen et al., 1998). Yet at the moment, they have not been applied to the full decomposition of a cognitive task at the whole-brain level. Part of the difficulty to achieve this is that three fundamental methodological issues have to be simultaneously resolved: (1) estimate timing information at a slow sampling rate, thus allowing to provide a whole-brain measure; (2) estimate timing parameters invariantly across different brain regions, independently of possible variations in the shape of the hemodynamic response function (HRF); (3) distinguish changes in onset latency and in duration (Bellgowan et al., 2003).

In addition to the solution of these methodological issues, a full parsing of a task requires a model of the expected sequence, to decompose the observed delays and durations in terms of contributions of the successive stages. In a serial scheme, the onset of the stage $\{i\}$ can be calculated as the sum of the onset and durations of stage $\{i-1\}$. This can be solved recursively to obtain the total organization of the task into subcomponents. However, questions such as the parallel or serial nature of the stages of a task are not fully understood and in a general cognitive task, the organization of processing stages may be highly complex, variable and unknown (Sigman and Dehaene, 2005).

Here, we introduce a novel strategy which solves the previously stated methodological difficulties and use it in a sequential task, where onset and duration of the processing stages are under experimental control. The strategy is based on previous Fourier-based methods (Lee et al., 1995; Menon et al., 1998; Rajapakse et al., 1998), and crucially, on the experimental manipulation of the task to differentially affect the timing of its successive stages. By studying the covariation of the timing parameters with the experimental manipulation, we achieve a measure which is insensitive to the particular shape of the HRF and thus invariant across the brain. With an algebraic estimation of these obtained parameters, we are able to recover the precise timing of all the stages which compose the task, which involves a large variety of cognitive processes. The duration

* Corresponding author. INSERM-CEA unit 562 "Cognitive Neuroimaging", Service Hospitalier Frédéric Joliot, Orsay, France.
E-mail address: sigman@df.uba.ar (M. Sigman).
Available online on ScienceDirect (www.sciencedirect.com).

1053-8119/$ - see front matter © 2006 Elsevier Inc. All rights reserved.
doi:10.1016/j.neuroimage.2006.05.064

of the whole task, composed of five stages, is less than one TR (the sampling time).

Experimental procedures

Simulations and calculation of predicted values of the phase

Simulations were performed by convolving square pulses of duration D and delay Δ with the HRF described in SPM99, using the default parameters: delay of response (relative to onset)=6 s, delay of undershoot (relative to onset)=16 s, dispersion of response=1 s, dispersion of undershoot=1 s, ratio of response to undershoot=6 s. We show here the analytic calculation of the value of the phase and the amplitude as a function of the critical parameters. The BOLD time-series is given by the convolution between the HRF and a time series representing the brain activation responses to N periodic presentations of a fixed stimulus (with period T). We assume that, for each stimulus $i=1{:}N$, the activation has fixed duration D and delay ϕ, but may exhibit trial-by-trial variability in amplitude A_j.

The Fourier transform of the BOLD signal is then given by the formula:

$$F(w) = \mathrm{HRF}(w) \cdot \sum_{j=1:N} \int_{j^*T+\phi}^{j^*T+\phi+D} A_j \cdot e^{-iwt} \mathrm{d}t$$
$$= \mathrm{HRF}(w) \cdot \sum_{j=1:N} A_j \cdot \frac{1}{-iw} \left(e^{-iw(j^*T+\phi+D)} - e^{-iw(j^*T+\phi)} \right)$$

HRF(w) notes the Fourier Transform of the HRF and we have made use of the fact that the Fourier transform of a convolution is just the product of the convolutions. All the terms that do not depend on j can be factored out, resulting in:

$$F(w) = |\mathrm{HRF}(w)| \cdot e^{-iw \cdot \arg(\mathrm{HRF}(w))} \cdot e^{-iw(\phi+D/2)} \left(\frac{e^{-iwD/2} - e^{iwD/2}}{-iw} \right) \times \sum_{j=0:N} A_j \cdot e^{-iwjT}$$

This can be rewritten as:

$$F(w) = e^{-iw(\phi+D/2+\arg(\mathrm{HRF}(w)))} \cdot |\mathrm{HRF}(w)| \cdot \frac{2}{w} \cdot \sin(wD/2) \times \sum_{j=0:N} A_j \cdot e^{-iwjT}$$

The last term (the sum), while complex for arbitrary frequencies, is real for the particular case of the frequency of stimulation, $w = \frac{2\pi}{T}$. Also, for this value of w, and for small values of D compared to T (as used in this experiment in which $D<1$ s and $T=15$ s) $\frac{w^*D}{2} = \frac{\pi^*D}{T} << 1$ and thus the previous equation may be simplified to:

$$\mathrm{F}(w) = e^{-iw(\phi+D/2+\arg(\mathrm{HRF}(w)))} \cdot |\mathrm{HRF}(w)| \cdot D \cdot \sum_{j=0:N} A_j$$

Hence, the phase at the stimulation frequency, which can be experimentally measured, is a constant plus $\phi+D/2$, i.e. directly reflects changes in onset and duration of brain activation. Note that the measurement is independent of the distribution of the A_j and thus is expected to be unaffected by amplitude noise. A constant factor is added to the phase by the contribution of the HRF. However, this factor will be cancelled out when the response to two different conditions are subtracted (because of its additive nature). Furthermore, we can also see that the amplitude is proportional to the mean amplitude of the stimulation and scales with the duration D. Note that the phase, $w^*(\phi+D/2)$ is a dimensionless quantity and corresponds to the value in radians of the cycle at the repetition time. For simplicity, however, throughout the manuscript we will express the value of the phase as a temporal delay relative to the inter-trial interval (in seconds), i.e. we report the dimensionless phase multiplied by $T/2\pi$. The scaling predictions are unchanged (w is always fixed) and the advantage is that this leads to a value which is expected to be independent of the stimulus repetition time.

We emphasize that in this analysis we are not using all the spectral information, only the value at the frequency of stimulation, which can easily be extracted from the BOLD response by correlation with two regressor functions (cosine and sine at the frequency of the stimulus). The Fourier analysis is merely used as an efficient means of mathematically describing our method.

Participants

Nine healthy human adults (mean age 22) participated in the fMRI study after giving written informed consent. All were right handed (Edinburgh Inventory) and had normal or corrected-to-normal vision. The study was approved by the regional ethical committee (Hopital de Bicêtre, France).

Procedure

The experiment was divided in eight blocks. The number of repetitions (n) was indicated before the beginning of the block and did not change throughout. Two blocks were performed for each value of n and the order of n across the different blocks was randomized within subjects with the requirement that the same n would not be repeated for two consecutive blocks. Each block consisted of 20 identical trials, and the ITI was set to 15 s. Thus, the total duration of each block was of 310 s; including 10 s at the beginning of each block which were discarded.

Stimuli and task

Subjects saw a video projector through a set of mirrors. Checkerboards covered the whole screen (about 20° of the visual field) and were presented during 125 ms, always in pairs of alternating phase (black becomes white and white becomes black). The task (see Fig. 2A) begins with a dimming of the fixation point, lasting 300 ms, thus alerting the subject about the beginning of the trial. Engagement of attention presumably constitutes a *first stage* of the task (labeled grey in the box scheme). Then, a series of pairs of contrast-reversing black-and-white checkerboards are presented. Each pair lasts 250 ms and the number of presented pairs varies according to the experimental parameter (n) which indicates the number of repetitions. Subjects are required to tap with the right hand in synchrony with the alternation of the checkerboard. Thus, the number of taps also follows the parameter n. This process of visuo-motor synchronization constitutes the *second stage* (labeled blue in the box, scheme). Note that the duration, but not the onset of this stage changes with n. Third, a word is presented in the center of the screen. Word reading constitutes the *third stage* (labeled green in the box, scheme). The onset, but not the duration of this stage changes with n. After the presentation of the word, subjects were instructed to internally rehearse the word n times, with a timing as close as possible to 250 ms per word. The rehearsal

process constitutes the *fourth stage* of the task (labeled yellow in the box, scheme). Both the onset and the duration of this stage change with (n). Once subjects finish rehearsing the word, they signal it by clicking a button with the left hand. If appropriately timed, their response should be synchronous with a loud trumpet sound which is presented at a fixed, reference latency. This last process of task conclusion constitutes the *fifth stage* (labeled red in the box, scheme). The duration, but not the onset of this stage change with (n). Words were chosen from a list of 20 different monosyllabic four-letter words, matched for frequency. French words were used and all subjects were native French speakers. The loud trumpet sound had a fixed, one-second duration and was presented at the time at which subjects were expected to finish the verbal rehearsal and execute the left button press. This time was set to be ($300+250*n$ ms) after the word presentation. The number of repetitions (n) was varied across blocks from 1 to 4 and the total task duration is ($600+500*n$ ms) which corresponds respectively to 1100, 1600, 2100 and 2600. Note that, in the case of longest duration, the whole task is of the order of TR, our sampling time. Between trials, a fixation cross remained in the screen and subjects were asked to fixate. Before entering the scanner, subjects were trained until they could perform the task reliably, without errors (errors within the scanner were less than 1% of the trials) and in a precisely timed manner.

fMRI parameters

The experiment was performed on a 3T fMRI system (Bruker, Germany). Functional images sensitive to blood oxygen level-dependent contrast were obtained with a T2*-weighted gradient echo-planar imaging (EPI) sequence (repetition time [TR]=2.4 s; echo time [TE]=40 ms; ANGLE=90°; field of vision [FOV]=192×256 mm; MATRIX=64×64). The whole brain was acquired in 26 slices with a slice thickness of 4.5 mm. High-resolution images (3D gradient echo inversion-recovery sequence; inversion time [TI]=700 mm; TR=2400 ms; FOV=192×256×256 mm; MATRIX=256×128×256; slice THICKNESS=1 mm) were also acquired.

Image processing and statistical analysis

FMRI data were preprocessed with SPM99 (http://www.fil.ion.ucl.ac.uk/spm/). The first 4 volumes were discarded. All other volumes were realigned using the first volume as reference, corrected for slice acquisition timing differences, normalized to the standard template of the Montreal Neurological Institute using an affine transformation, and spatially smoothed (6 mm).

Since the acquisition is asynchronous and thus the frequency of repetition time is not an integer value of the number of scans, we calculated the phase and amplitude by projecting the time signal to a *cosine* (*cos*) and a *sine* (*sin*) functions. For each voxel within each session, to avoid numerical instabilities, we detrended the raw signal (corrected for linear drifts and subtracted the mean). We then estimated for each voxel j the projections: $A^j x = \sum_i s_i \cdot \cos\left(\frac{2\pi \cdot \mathrm{TR} \cdot i}{\mathrm{ITI}}\right)$ and $A^j y = \sum_i s_i \cdot \sin\left(\frac{2\pi \cdot \mathrm{TR} \cdot i}{\mathrm{ITI}}\right)$ where $\{S\}$ corresponds to the detrended signal, and j the voxel number. ITI was 15 sec, and TR 2.405 sec. Then, phase and amplitude were calculated as $\phi^j = \arctan\left(\frac{A^j y}{A^j x}\right)$ and $A^j = \sqrt{(A^j x)^2 + (A^j y)^2}$.

To identify the network of voxels engaged in the task, we used phase information and estimated the fraction of measurements of the phase that lied within the expected response range (ERR). A total of 72 measurements were obtained (all the acquired session were considered for the analysis) corresponding to 4 conditions, each repeated for 2 sessions, for 9 subjects. The ERR was set to the interval from 4 to 10 s, based on previous characterizations of the HRF and allowing a margin to account for region-to-region variability and changes across conditions (we expected a maximum 2 s difference between the slowest and fastest condition). The probability that x out of 72 measurements lie within the ERR can be calculated following the binomial distribution. $f(x,72,p)$ where $p=0.4$ is the fraction of ITI occupied by the ERR duration (6/15 s) and thus the probability of success for a single random value. The probability that by chance more than x out of this 72 measures fall within the correct window is given by the cumulative distribution $F(x) = \Sigma_{i>x} f(i,72,p)$.

In this study, we performed a whole-brain analysis and are thus confronted with the problem of multiple statistical comparisons. To largely reduce the occurrence of Type II errors, we used extremely severe statistical criteria, setting the minimum number of sessions within the ERR to (68/72) (95%). The probability that a voxel has a value of the phase within the ERR on more than 95% of the measured values, following the cumulative binomial distribution, is $p<10^{-22}$.

For all active voxels within the active region, we calculated the value of the phase and of the amplitude for all n. We then calculated the value of the slopes for amplitude and phase. The slope of the phase is expressed in milliseconds. The value of the amplitude is proportional to the intensity of the EPI images which varies from region to region, depending on tissues and other anatomical and imaging factors unrelated to neuronal activity. To avoid a signal biased by the mean contrast of the EPI image, we estimated, for the amplitude measurement the regression coefficient r which provides an unbiased estimate of the covariation between amplitude and n. This was done for the 18 different experimental sessions (2 repetitions×9 subjects) and all the data were averaged across subjects and sessions. From the resulting images of mean value of the slope for the phase and mean r for the amplitude, we identify the different stages following the sketch in Fig. 2. A voxel was labeled as belonging to State i if the measured slope (averaged across subjects and sessions) and the predicted slope did not differ in more than 125 ms, and if the measured r did not differ in more than 0.5 from the expected value for this stage. None of the main results were qualitatively dependent on the precise window chosen for assigning a voxel to a given stage. Finally, for all the identified clusters, we performed paired t tests to measure the significance of the difference in the phase measurements across the different values of n. This was done by collapsing all the voxels of the cluster into a single value, for each experimental session. A t test for all possible combinations (a total of 6) was done by comparing the obtained values for all different sessions. Since the measurements for the different voxels within each cluster were highly correlated, choosing the most active voxel instead of the mean across the entire cluster yielded essentially equivalent results.

Results

An analytic method to obtain timing information from the fMRI signal and to identify sequential stages of processing

In this section, we describe the basic aspects of our analytic method, as well as simulations designed to estimate the optimal parameters. We extract the spectral parameters, *amplitude* and *phase*, from the BOLD signal resulting from a slow periodic

stimulation set by the inter trial interval (ITI). While the absolute value of the phase and spectrum depends on various parameters such as the HRF, or the repetition frequency, their relative value (i.e. the comparison of these values in two different conditions) follows a precise prediction based on changes in duration and onset of the response. The crucial aspect for this analysis is the manner in which these measurements vary with the experimental manipulations. For consistency with the experimental results, in Fig. 1, changes in delay and duration are plotted in function of the scaling parameter $n=250$ ms. A change in the onset of the response (referred as delay or ϕ) changes the phase linearly, and with a slope of 1, and has no impact on the amplitude (Fig. 1, first row). A change in the duration of the response also affects linearly the phase, but with a slope of 1/2 (intuitively, because the center of mass is shifted by half the width) and results in a linear increase, with a slope of 1, in the amplitude (Fig. 1, second row). These operations are linear and hence (within a regime in which the response itself behaves linearly) combinations of these effects summate. Thus, a change in delay Φ and in duration D will result in an increase of the phase of $\phi+1/2*D$ and the change in the amplitude will be proportional to D (Fig. 1, third row, and see Experimental procedures for a proof). The amplitude of the spectrum will only be affected by changes in duration, but will remain unchanged by different delays.

In summary, by studying the covariation of the phase and the amplitude with different experimental manipulations, the changes in Φ and D may be estimated. While relying on the assumption of the stationary character of the signal (Aguirre et al., 1998) and linearity of the response (Boynton et al., 1996), the advantage of this approach is that the contribution of the HRF to the phase is factored out from the timing differences (see Experimental procedures). Thus, the estimate is independent of the particulars of the HRF at different brain sites, and does not require a specific model of the shape of the HRF. In addition, the phase measurement is completely insensitive to amplitude noise (see Experimental procedures for a formal demonstration).

Prior to the experiments, we estimated in simulated fMRI data the parameter values for which phase and amplitude are optimally estimated. It is not the objective of this study to provide a detailed result of the exploration of the parameter space, but we do note two important factors. First, there is a compromise in the choice of the inter-trial interval (ITI): as ITI decreases, more trials are acquired (keeping scanning time constant) but trials are less independent and the phase estimates worsen. We find that for typical experimental times (~30 min of scan time) the best inter-trial interval (ITI) is within the 11–16 s range. Second, there is an obvious effect of TR, with a worse estimation as TR increases. However, the most critical factor is a sharp increase in estimation error for values of the TR which corresponded to a rational fraction

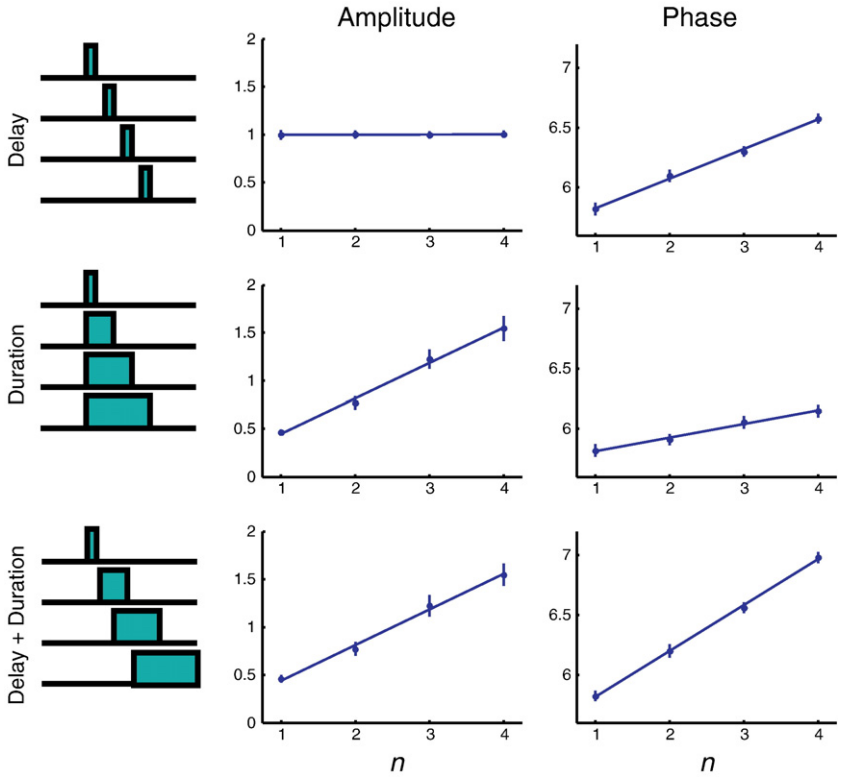

Fig. 1. Spectral analyses of the BOLD signal can dissociate changes in onset time and in duration of brain activation. Changes in the onset and in the duration of the response can be measured by analyzing the amplitude and the phase of the BOLD signal in response to a slow (14 s) periodic stimulation. For consistency with the experimental results, changes in delay and duration are plotted in function of the scaling parameter $n=250$ ms. A change in delay (first row) results in a linear increase of the phase (with a slope of 1) but does not change the amplitude. A change in duration results in a linear change of slope 1/2 in the phase (intuitively because the center of mass is shifted by half of the duration value) and a change of slope 1 in the amplitude (second row). These effects are additive, allowing to detect simultaneous changes in onset and duration (third row). All figures correspond to simulated data with standard BOLD parameters (see Experimental procedures for details and for analytical proofs of these results).

of the ITI. In essence, acquisition asynchronous with the presentation time allows an oversampling of the HRF, thus achieving better time resolution. The values of TR (2.405) and of ITI (15 s) were chosen from these preliminary simulations.

Task design, experimental manipulations and behavioral results

We designed a rhythmic task, which involves a sequence of perceptual, motor and verbal operations composed of five stages. The details of the task are described in Experimental procedures and in Fig. 2A. Here we refer to issues in the logic of the design which are fundamental for our analysis. The task was varied according to an experimental parameter henceforth referred as *Number of Repetitions* or simply as n which controls the number of repetitions of certain stages of the task. This results in the stretching (increased duration) of such stages and in the delay of the processes which follow them in sequential order. Different stages involved sensory stimulation, motor action or both. Subjects were required to precisely time their actions, including motor taps (Stage 2, right hand, and Stage 5, left hand) and the internal rehearsal of a word (Stage 4). After a few training sessions, subjects reached a reliable performance (Fig. 2B).

The timing of the different stages was differentially affected by the number of repetitions (Fig. 1). Our task included a stage for which neither the duration nor the onset changed with n (Stage 1); a stage for which only the duration increased with n (Stage 2); two stages for which only the onset, but not the duration, increased with n (at different rates: Stages 3 and 5); and finally, a stage for which both the duration and the onset increased with n (Stage 4). The value of the onset and of the duration as a function of n is illustrated in Fig. 1. We next show that by studying this covariation, we can actually identify the brain regions which participate in each stage.

Following the predictions sketched in Fig. 1, a change in delay ϕ and in duration D will result in a increase of the phase of $\phi + 1/2 * D$, and the change in the amplitude will be proportional to D. Thus, for each stage we can predict the quantitative value of the slopes of covariation of fMRI phase and amplitude with n. These predictions are summarized in Fig. 2. For amplitude measurements, to avoid a response biased by the local contrast of the echoplanar images (EPIs) we calculated the regression coefficient r, which follows a similar prediction (1 for stages that change in duration with n, and 0 for stages that do not change in duration).

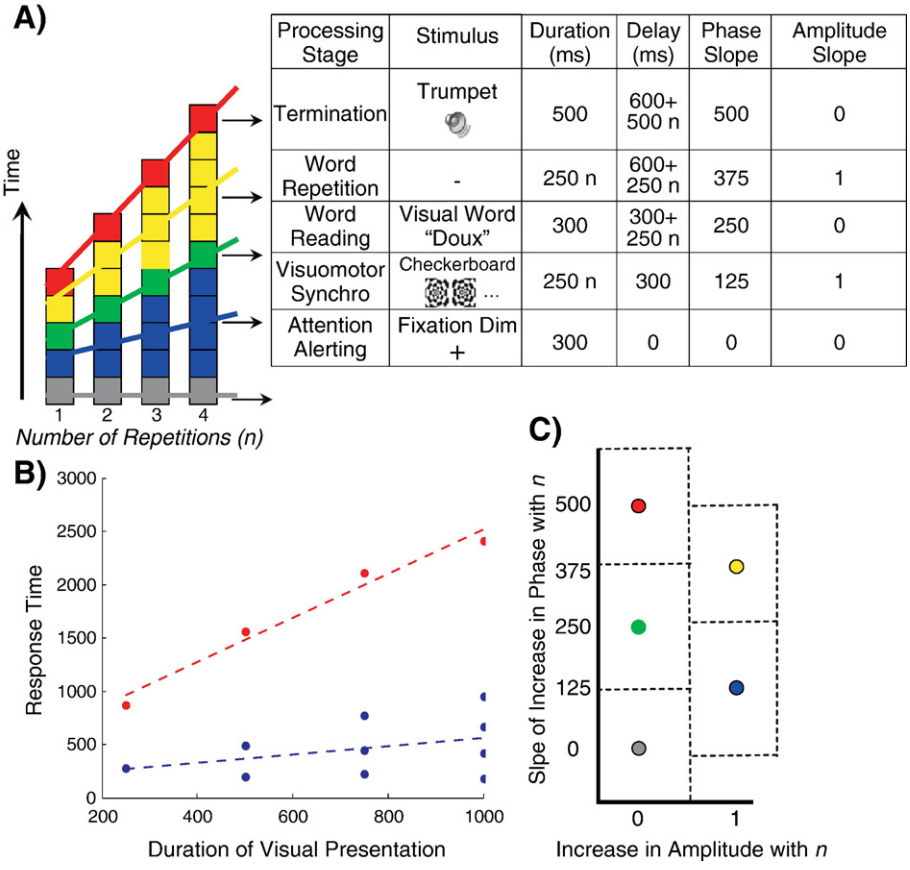

Processing Stage	Stimulus	Duration (ms)	Delay (ms)	Phase Slope	Amplitude Slope
Termination	Trumpet	500	600+ 500 n	500	0
Word Repetition	-	250 n	600+ 250 n	375	1
Word Reading	Visual Word "Doux"	300	300+ 250 n	250	0
Visuomotor Synchro	Checkerboard ...	250 n	300	125	1
Attention Alerting	Fixation Dim +	300	0	0	0

Fig. 2. Sketch of the experimental paradigm, behavioral performance and predicted covariations of BOLD signal with experimental manipulations. (A) Schematics of the 5 stages composing the sequential task and how their duration and onsets covaries with the experimental factor (n). (B) Behavioral results. Right-hand responses (synchronized with the checkerboards) are shown in blue (for the repeated conditions, the timing of all successive taps are indicated by the blue dots) and left-hand responses (to terminate the trial, synchronized with the trumpet sound) are shown in red dots. Regression lines are shown for both conditions. (C) The predicted value for the slope of the change of the amplitude and the phase of the signal with (n) for the five stages (calculated analytically as shown in Experimental procedures). This predicted value is used to identify the brain regions associated with each processing stage.

Identifying the task-related network

We first identify the regions of the brain which participate in the task, regardless of their timing, using a spectral method which proves to be very consistent and reaches very high standards of significance. While the precise value of the phase may vary across regions and conditions, this variability should be within an expected response range (ERR) of 4–10 s, based on characterizations of the HRF (Miezin et al., 2000). We thus counted for each voxel the percentage of time that the measured phase (out of 72 sessions including all subjects and conditions) was within the ERR. The probability that by chance *more* than *x* of these 72 measures fall within the correct window is given by the cumulative binomial distribution (see Experimental procedures for details) The fraction of sessions with a phase in the ERR reflects a very clear structure. A massive number of voxels are seen at 40%, with a very broad distribution of phases. This value corresponds to the mode expected for random data and thus is consistent with task-independent voxels, either because they do not lie within grey matter or because they cover regions which do not respond to the task. Starting at 80% and increasing up to 100%, a second cluster is observed, of voxels with a sharp phase distribution close to the expected response value. A very selective criterion was established to identify task-responsive voxels, considering only voxels for which 95 percent, i.e. 68 out of a total of 72 sessions (including all subjects and conditions for each subject), had a value of the phase within the ERR. The probability of type II errors, i.e. that this criteria is satisfied by chance (determined by the binomial distribution, in green), is $<10^{-22}$. None of our main findings is dependent on the precise choice of the threshold. We also identify a set of voxels for which their phase is systematically out of this range (left portion of the distribution of Fig. 3A) In our experimental data, an important proportion of voxels (2.8%) satisfies this criterion. The activated regions involve a mostly bilateral and extended network which covers occipital cortex (striate and extra-striate), the intra-parietal sulcus (IPS), the auditory regions in the temporal lobe (including primary regions in Heschl's gyrus, and more dorso-lateral regions in the suparmarginal gyrus, the thalamus, inferior frontal cortex and the insula. We will consider this network for all further analysis (unless explicitly stated). Interestingly, a highly significant proportion of voxels (1.5%) was found whose phase values very rarely fell within the ERR (<5% of phase measurements; the probability that this may result from chance is $p<10^{-11}$). We speculate that these voxels may correspond to regions which deactivate upon task presentation, thus inducing a phase shift of half of the ITI and the phase falling systematically outside of the ERR. We generated anatomical maps assigning to each voxel the percentage of sessions for which the value of the phase was within the ERR (Fig. 3). The regions with low values correspond precisely to those described as deactivating in a systematic fashion during a large variety of tasks (Gusnard and Raichle, 2001). While we do not pursue a systematic analysis of deactivated regions, this finding provides a good measure of consistency of our method.

Parsing the task into sequential stages

Having identified task-responsive regions, we next performed the timing analysis. In Fig. 4 we illustrate the process leading from the BOLD signal to the extraction of timing information, with two examples from the auditory and visual cortices. The power spectrum showed a clear maximum at the stimulation frequency, which was evident for all active voxels.[1] We then calculated regression slopes for the changes in amplitude and in phase as a function of the number of repetitions (*n*). Finally, we calculated the voxel's processing stage following the scheme described in Fig. 2. A voxel was attributed to a stage (1–5) if the absolute value of the difference between measured and predicted values was not larger than 125 ms for the phases, and than 0.5 for the amplitudes.

The results of this analysis, performed across all voxels within the active network, appear in Figs. 5 and 6 and in Table 1. All the active clusters for which we had a prior expectation are classified in their predicted stage. A large cluster in the occipital lobe and one in the left motor cortex belong to Stage 2, which corresponds to the right hand tapping in synchrony with the alternating checkerboards. The primary auditory cortex and the right motor cortex, two other brain regions for which there was a clear prediction, are classified as expected, in Stage 5. For both of these stages, we observe a more accurate and reliable measurement for the sensory than for the motor cortices. The standard errors of the slope of the phases of motor cortices show an almost twofold increase (for Stage 2, 32.5 ms vs. 85 ms for the visual and motor clusters; for Stage 5, 64 and 70 ms for left and right auditory cortices vs. 102 ms for the motor cortex). In addition, the slope of the phase of the left motor activity was 430 ms, slightly smaller than the predicted value of 500 ms. This may indicate the presence of earlier motor activation, either due to early motor preparation or to a spill-over of activation from the left and right hands. We also identified a cluster belonging to Stage 2, lateral and inferior to the motor activation, and also lateralized to the left (Talairach Coordinates [−60, 16, 24]). Its localization fits within an activation of the secondary somatosensory area SII (Frot and Mauguiere, 1999) accompanying the finger taps.

The auditory and right motor regions were the only clusters belonging to Stage 5. However, when analyzing activation at a lower threshold ($p<10^{-13}$), we observed two bilateral clusters in the ventral striatum (coordinates [10, 22, 0] and [−18, 24, 2]) which correspond to Stage 5. The ventral striatum activations may signal the termination of the sequence, although we cannot disambiguate whether they relate to a striatal control of sequential stages (Doyon et al., 1996), a measure of reward (Robbins and Everitt, 1996) related to conclusion of the task, or an interaction between these factors (Graybiel and Kimura, 1995; Koechlin et al., 2002; Schultz et al., 1995).

Stages 3 to 5 involve a series of different processes which belong to the auditory-verbal network. Stage 3 involves the recognition of a visual word and its the transformation to an internal phonemic or articulatory code; Stage 4, the rhythmic rehearsal of the presented word; and Stage 5, the sensory response to a complex sound. We find an organization in the superior temporal lobes which reflects this parsing. In the right superior temporal cortex, we see only activations around Heschl's gyrus, corresponding to primary and secondary auditory areas appropriate to Stage 5. In the left hemisphere, however, we observe a gradient from medial-anterior to lateral-posterior regions within the superior temporal lobe, with a transition from Stage 5, to Stage 3 and then to Stage 4, which is consistent with a hierarchical organization of auditory areas (Scott and Johnsrude, 2003) given by the

[1] Actually, the anatomical map resulting from the ratio of the amplitude at the stimulation frequency and the mean value in the neighboring frequencies (a measure of the noise in the signal) is very similar to the activation map, except that the sign is lost and the statistics are not as significant.

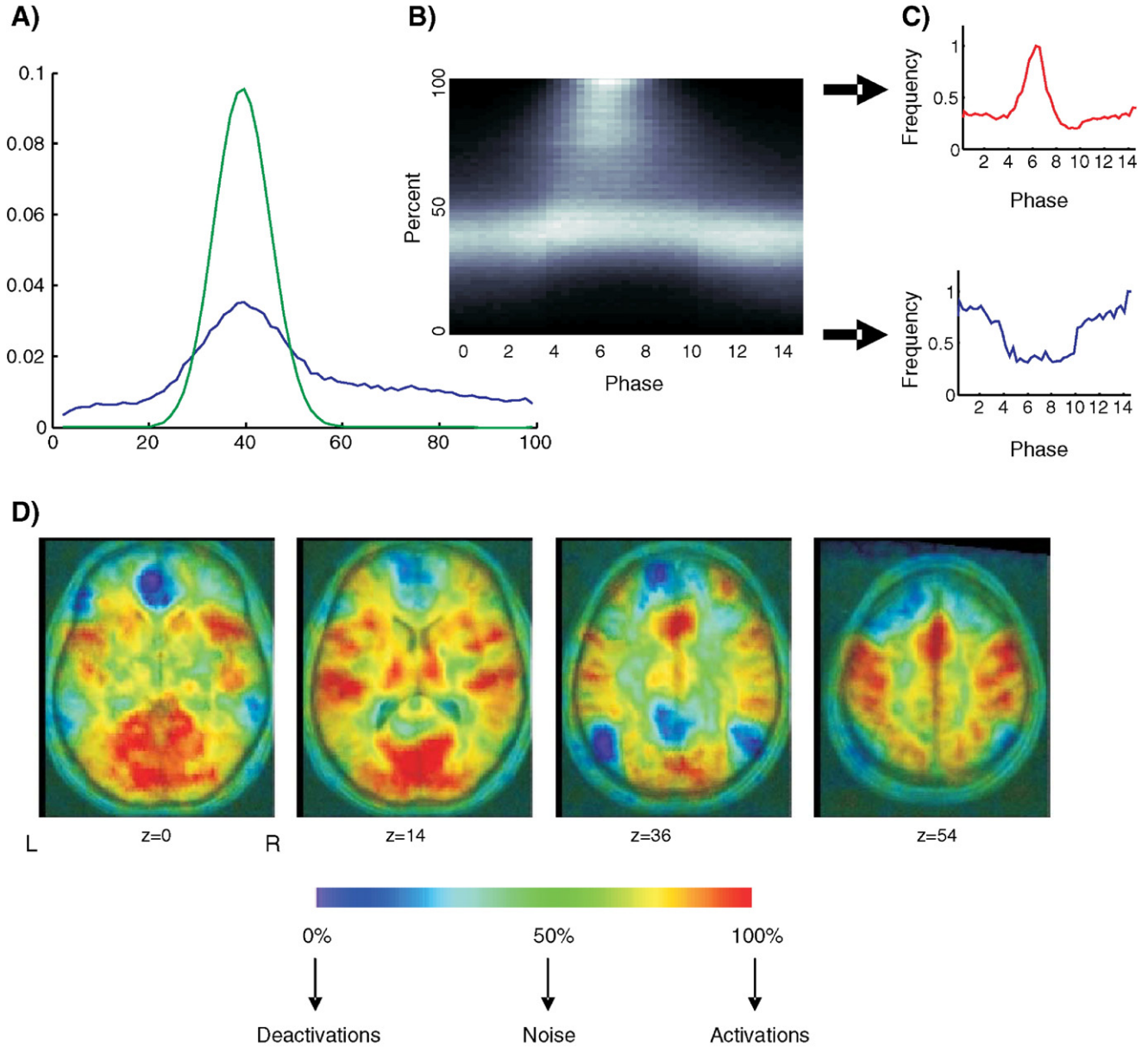

Fig. 3. Extracting task-relevant brain regions based on phase information. (A) Fraction of sessions for which the value of the phase lies within an expected response range (ERR, see Experimental procedures) of 4 to 10 s. The experimentally obtained distribution (blue line) is to be compared with the expected values of a random data set, determined by the binomial distribution (green line). (B) The distributions of phases for voxels as a function of the percentage of sessions for which the phase lie in the expected response interval. (C) The histogram of phases for the voxels in which >95% of the sessions is within the ERR (Red line) and those for which <5% is within the ERR (blue line). The phase value of the latter voxels is a half-period (i.e. 7.5 s) away from the expected value, suggesting that they inactivate during task execution. (D) Brain regions which show phases consistently within the ERR (active regions) are shown in red and brain regions whose phase is consistently out of the ERR (inactive regions) are shown in blue. Four axial sections at values of z-Talaraich coordinate of 0, 14, 36 and 54 mm (going from the left to the right panel) summarize the main regions involved. In the two more ventral slices ($z=0$ and $z=14$), the active regions include visual cortices (striate and extra-striate), auditory cortices, thalamus and inferior frontal cortex. A cluster in the medial portion of inferior frontal cortex had values of phases systematically outside of the ERR, indicating that this region is deactivated during the task. In the two posterior slices ($z=36$ and 54), posterior parietal (PP), motor, premotor (Supplementary Motor Area, SMA) and frontal cortices are activated by the task. The posterior cingulate (PC) and the angular gyrus are deactivated.

correspondence Stage 5 – Pure Sound, Stage 3 – single word, Stage 4 – word rehearsal. In addition to the most posterior regions of the superior temporal lobe, Stage 4 also involves the right infero-temporal cortex, the anterior cingulate and the cerebellum (see Fig. 5 and Table 1). While prominently lateralized to the right, the inferior frontal activation is bilateral at a lower threshold ($p<10^{-13}$). This lateralization is consistent with findings that show that, while most language processing is left lateralized (Binder et al., 2000), the rhythmic and prosodic components of speech are frequently right lateralized (Fries and Swihart, 1990; Riecker et al., 2002).

Since Stage 3 involves visual word recognition, we also expect to observe a left-lateralized activation of the occipito-temporal sulcus, at the site responsive to the visual form of words (Cohen and Dehaene, 2004). Indeed, at lower threshold ($p<10^{-13}$), we

observed a small cluster (12 voxels), overlapping with previously described coordinates for the vWFA [−40, −57, −8] corresponding to Stage 3. We did not see a corresponding cluster in the right hemisphere.

At the highest threshold ($p<10^{-22}$), we did not see activations corresponding to Stage 1. However, when lowering the threshold ($p<10^{-13}$) we observed bilateral activations in the parietal cortex, and right activation in premotor regions (Fig. 6). These regions are active across all conditions, and neither the phase nor the amplitude changes with repetition number, indicating that they correspond to Stage 1. Parietal and premotor regions have been involved in the planning of motor action, such as reaching or

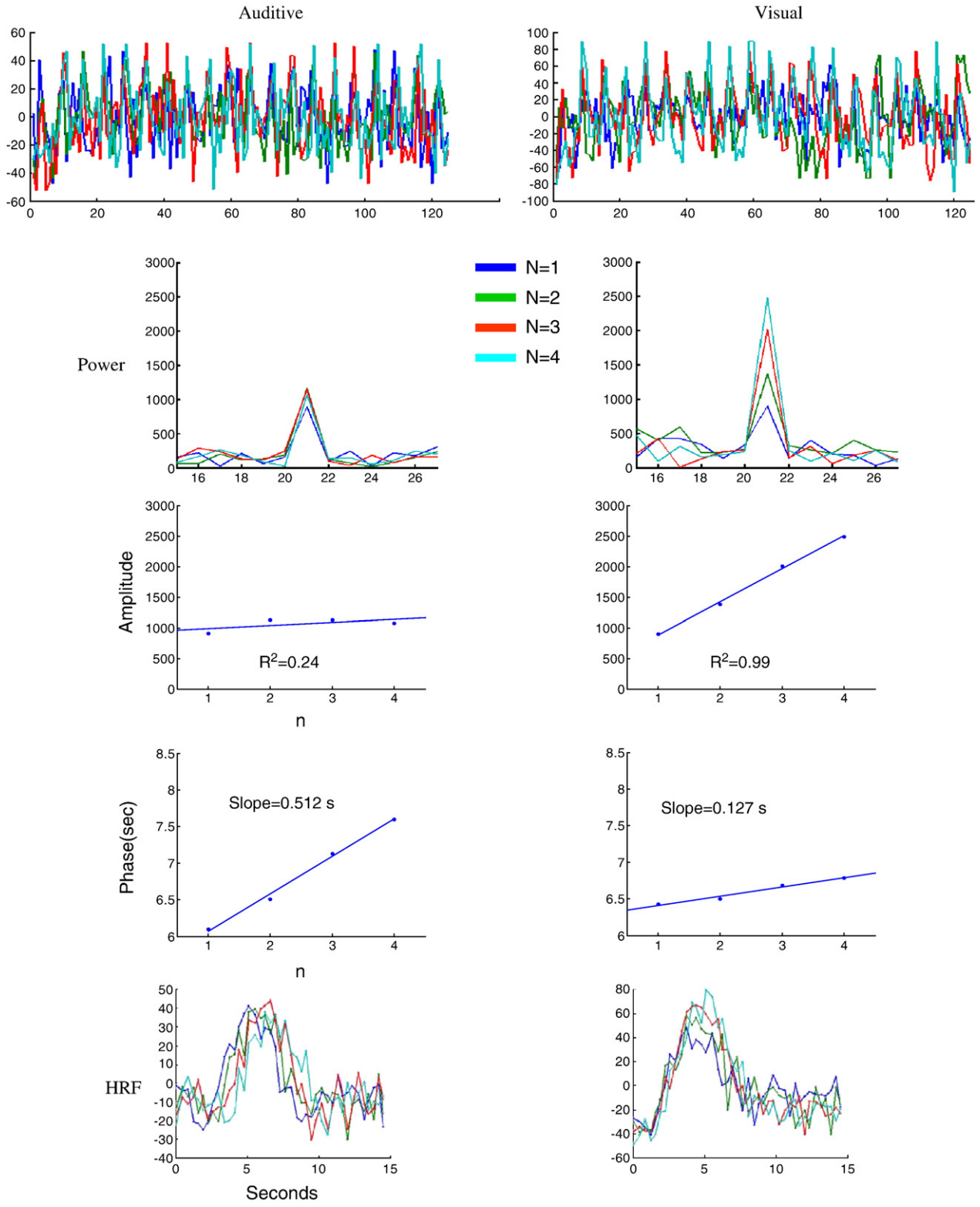

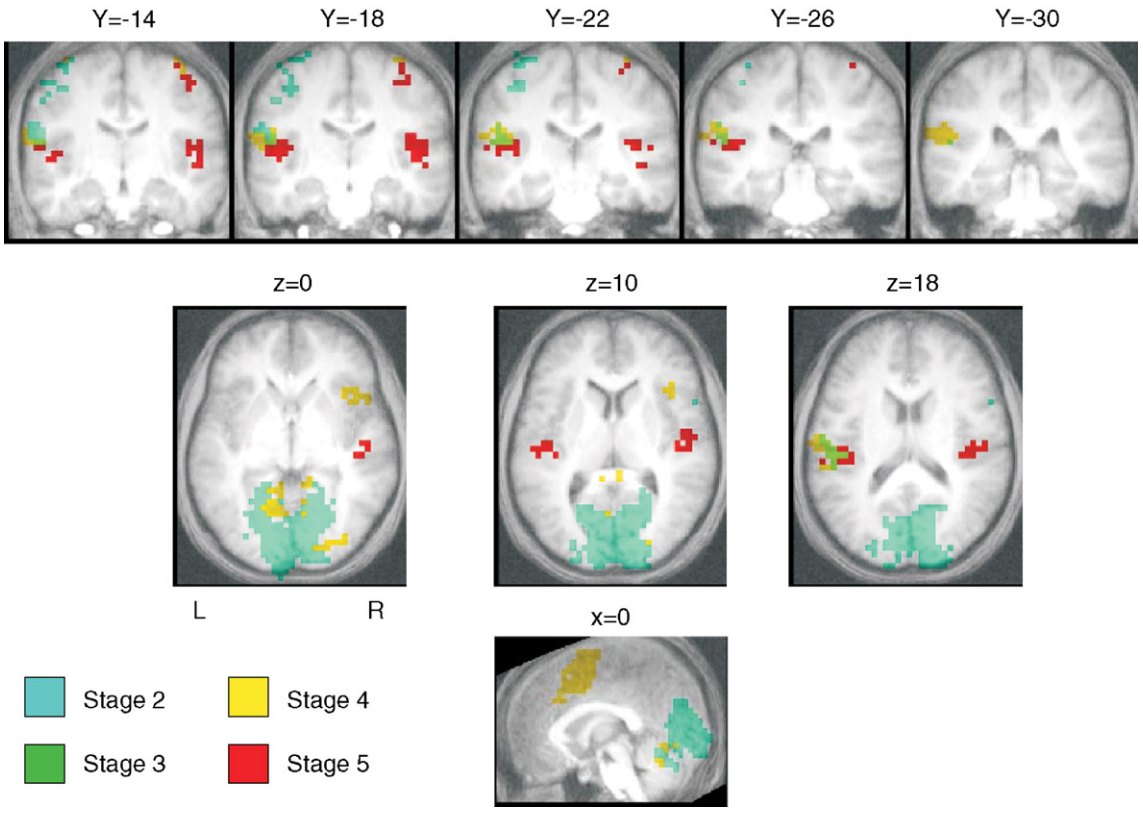

Fig. 5. Identification of brain regions active during the different stages of the task. Coronal, axial and sagittal slices show all the active regions, color-coded to indicate the corresponding processing stage. All sensory motor regions are classified at their expected stage. The coronal slices show an asymmetric activation in the superior temporal lobe, consistent with the recruitment of language mechanisms at stages 3 and 4. While on the right, there are only responses to the trumpet sound (corresponding to Stage 5) on the left there is a progression showing regions active during the word presentation (Stage 3) and during verbal rehearsal (Stage 4).

saccades (Andersen, 1995; Colby et al., 1996). Here we find that they are involved early in the preparation of a complex task which involves manual and verbal actions. These regions may also be involved in memory for the number of repetitions (Dehaene et al., 1999; Eger et al., 2003), a critical parameter of the task, that subjects memorized for one block and therefore had to bring to mind just prior to task execution.

A more detailed analysis of the phases of these clusters (Fig. 6) shows that while the relative differences in phases across conditions result in a consistent measurement, the raw value of the phase is not much informative, as expected if the HRF shape varies across voxels. For example, the phase for $n=1$ for right primary auditory cortex (Fig. 6, bottom right, Stage 5) is 750 ms faster than that for left posterior parietal cortex (Fig. 6, top left, Stage 1). This difference is opposite to the order imposed by the task, where auditory stimulation comes last. It is probably due to a slower HRF in parietal association cortex than in primary auditory cortex. Note that our analysis is based solely on *differences* in phase as n varies and is able to recover the expected ordering of activation in these regions. This ordering only becomes apparent in the raw phases when $n=3$ or 4, i.e. when the task delays are in excess of 1 or 2 s and dominate variations in HRF latency. Below this value, the spectral analysis is indispensable.

Similarly, from the analysis of the slopes in Fig. 6, it can be seen that the y-intercept of the amplitude slope is usually not zero. This is in apparent contradiction with the simple prediction of Fig. 1 (second and third row, in the simulations in which the duration is zero for $n=0$), which suggests that there should be no task-related activity when extrapolating to $n=0$. However, the finding of a significant intercept can be modeled as a baseline activity, related to the preparation of task-appropriate circuitry, and which is not modulated by the duration of subsequent stages. Indeed, some of

Fig. 4. Observed dissociation between changes in onset time and changes in duration in sensory cortices. (A) The raw signal (only corrected for a linear trend) is shown for all conditions for two sample voxels in primary auditory cortex (left column) and in primary visual cortex (right column). (B) The Fourier transform of these time series shows a clear maximum of the amplitude at the stimulation frequency. This maximum was evident for all active voxels. (C) The amplitude of the voxel in visual cortex increases linearly with n, but the amplitude of the voxel in the auditory cortex does not increase significantly with n. (D) Both voxels show a progression of the value of the phase with n, for the auditory voxel, the value of the slope is 512 ms and for the visual cortex it is 127 ms. Thus, based on the scheme of Fig. 2, the auditory voxel is classified within Stage 5 and the visual voxel within Stage 2. (D) For all conditions, we reconstructed the HRF from the original signal by locking all the times to the stimulus presentation and binning all the data in 300 ms windows. In this particularly simple case, the effects of delay and duration are evident from a simple inspection of the HRF. In non-primary cortices, however, the HRF was much noisier and thus only the proposed spectral analysis was able to recover changes in activation timing.

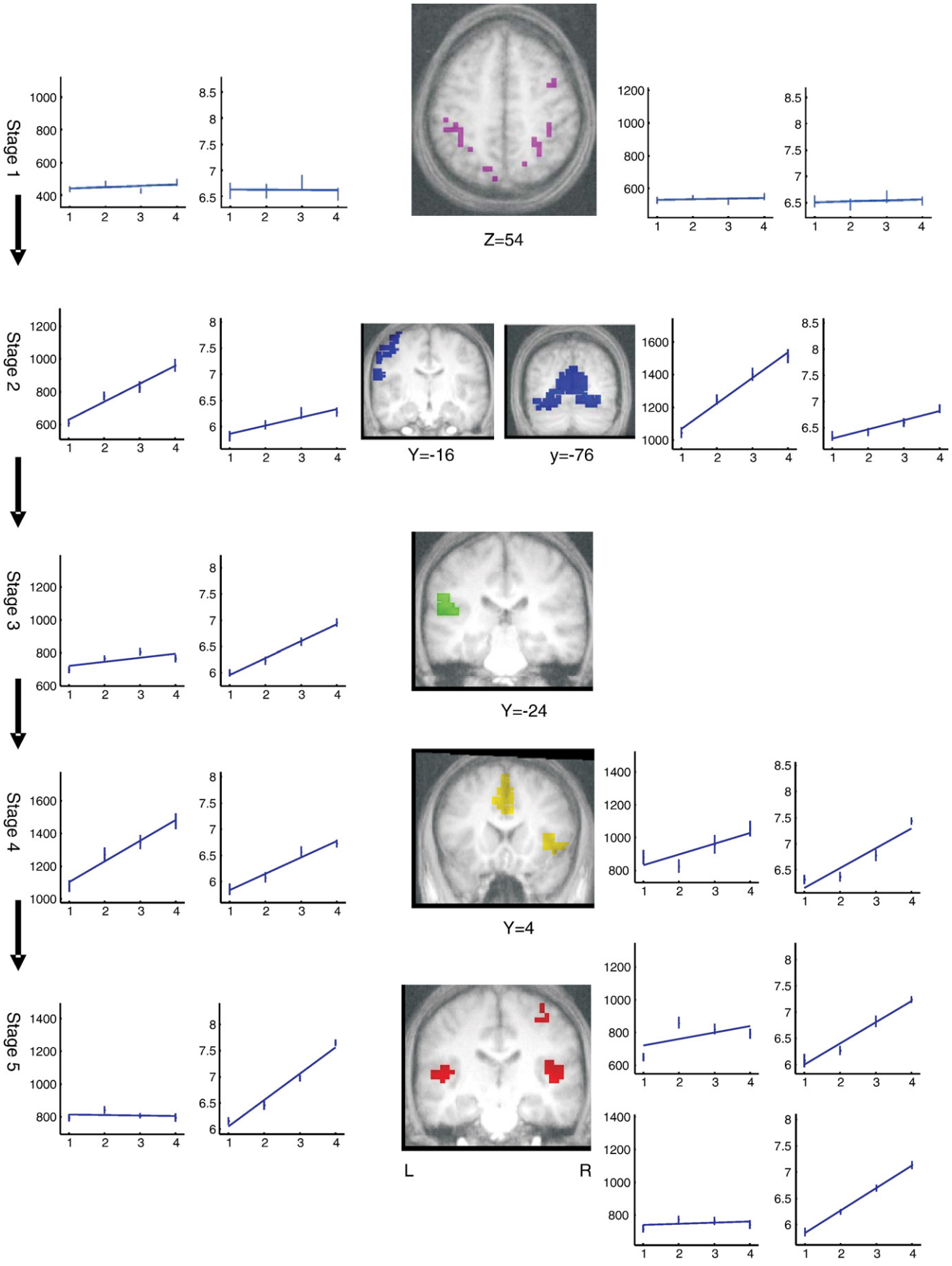
Stage 1
Z=54
Stage 2
Y=-16
y=-76
Stage 3
Y=-24
Stage 4
Y=4
Stage 5
L
R

Table 1

Stage			Anatomical region	Voxels	Slope of phase (ms)	SE (ms)	Spearman r for phase	Spearman r for amplitude	P value for difference in phase (and expected values of the difference in milliseconds)					
x	y	z							1 vs. 2	2 vs. 3	3 vs. 4	1 vs. 3	2 vs. 4	3 vs. 4
1					Expect: 0 ms		Expec 0	Expec 0	0 ms			0 ms		0 ms
53	11	19	Inferior frontal gyrus	12	13	100	0.119	0.053	0.995	0.996	0.208	0.356	0.067	0.523
32	−42	49	Posterior parietal (L)	10	−4	92	0.140	0.037	0.795	0.335	0.728	0.678	0.734	0.970
−41	−37	54	Posterior parietal (R)	16	69	139	0.003	0.060	0.992	0.431	0.469	0.667	0.843	0.868
2					Expect: 125 ms		Expec 1	Expec 1	125 ms			250 ms		375 ms
−60	−17	24	Postcentral gyrus (L)	14	158	77	0.682	0.908	0.496	0.208	0.061	0.524	0.012	0.013
−44	−16	59	Precentral gyrus (L)	44	148	84	0.916	0.964	0.335	0.134	0.883	0.071	0.090	0.033
1	−72	4	Occipital cortex	676	157	32	0.945	0.978	0.544	0.187	0.035	0.075	0.000	0.000
3					Expect: 250 ms		Expec 1	Expec 0	250 ms			500 ms		750 ms
−55	−26	15	Superior temporal gryus	16	301	60	0.990	0.266	0.147	0.059	0.029	0.000	0.000	0.000
−40	−57	−8	Fusiform gyrus (L)	12	205	48	0.889	0.363	0.404	0.780	0.028	0.807	0.007	0.012
4					Expect: 375 ms		Expec 1	Expec 1	375 ms			750 ms		1125 ms
26	−84	−1	Occipital cortex extrastriate	18	331	37	0.971	0.900	0.003	0.288	0.022	0.001	0.000	0.000
41	18	3	Insula (R)	18	367	67	0.886	0.781	0.825	0.114	0.015	0.057	0.000	0.000
−45	−5	61	Precentral gyrus (L)	22	328	69	0.911	0.952	0.058	0.039	0.915	0.004	0.005	0.000
44	−7	61	Precentral gyrus (R)	36	326	68	0.876	0.848	0.949	0.000	0.254	0.000	0.000	0.000
−60	−27	20	Superior temporal gyrus	38	343	55	0.962	0.913	0.116	0.041	0.006	0.001	0.000	0.000
−1	8	53	Anterior cingluate	121	326	48	0.962	0.968	0.110	0.002	0.232	0.000	0.000	0.000
−11	−57	−7	Cerebellum (L)	140	326	47	0.996	0.972	0.103	0.058	0.076	0.000	0.000	0.000
5					Expect: 500 ms		Expec 1	Expec 0	500 ms			1000 ms		1500 ms
40	−16	60	Precentral gyrus (R)	14	430	105	0.971	0;262	0.488	0.016	0.038	0.000	0.000	0.000
47	−17	11	Superior temporal gryus (R)	27	469	67	0.972	0.001	0.042	0.003	0.000	0.000	0.000	0.000
−48	−22	11	Superior temporal gryus (L)	31	472	71	0.999	0.062	0.049	0.001	0.027	0.000	0.000	0.000

the components of the task (for example the dimming of the fixation cue) do not scale with n and thus would be present even in the case $n=0$.

The measured slopes and their standard errors, which appear in Table 1, provide indications as to what differences in the mean time of activation are detectable across pairs of conditions. We ran paired t tests for all the different conditions to assess the significance of the phase measurement across subjects and thus to estimate the achieved temporal resolution. While the minimal resolution is variable from region to region, with motor regions more difficult to resolve than sensory regions in the present paradigm, differences are detectable whenever they exceed 250 ms, thus in the order of one tenth of TR, the sampling time. Note that this precision was obtained with only 40 measurements per subject in each condition. Thus, the precision is only indicative and would be expected to improve if more measurements were available.

Discussion

We have shown that we can parse a sequence of brain activations, using whole brain fMRI at a resolution of a few hundredth milliseconds, about 10 times better than the sampling time. While here we used the phase information in a periodic signal to obtain timing information from the fMRI (Menon et al., 1998), this does not seem to be essential and other proposed methods, which achieve comparable resolution could have been used (Bellgowan et al., 2003; Formisano and Goebel, 2003; Henson et al., 2000). The main novelty of our work consists in recovering the full sequence of activations in a sequential task in which the stage

Fig. 6. Quantitative measurement of the covariation of amplitude and phase with the number of repetitions for all the different stages. Each row corresponds to a different processing stage, with time increasing from the top to the bottom of the figure. Within each row, the anatomical localization of clusters being active during this stage (not all are included) is shown and immediately next to each cluster, a plot with the measured values of phase and another with the measured values of the amplitude for all values of n. All values correspond to means across the active cluster, and error bars correspond to the average standard errors. The regression line is plotted in all graphs.

order and duration of each stage are under experimental control. To achieve this, we solved simultaneously three critical issues: (1) invariance across different brain regions by providing a measure independent of the HRF; (2) a quantitative analysis of these variations which allows to distinguish changes in onset latency and in response duration and (3) due to the controlled nature of the task and thus having a precise model of the sequence ordering, we were able to use this information to reconstruct the order of activations within the task.

The two fundamental assumptions of our method are the linearity and the stationary nature of the hemodynamic response. While previous research provided evidence for these hypotheses (Boynton et al., 1996), our empirical finding that we can parse the different stages of a sequence with a linear method suggests that while non-linearities may be present, within the range of our experimental settings, their effect is moderate. Still, this linear analysis is bound to have a limit, for instance due to saturation of the response. For long-lasting activations, the response (neuronal and vascular) is likely to saturate. The dependence of the amplitude and of the phase with duration should therefore reach an asymptote, leading to a slope smaller than expected (1 for amplitude and 1/2 for the phase). Even though one could model this non-linearity and extend this analysis to more generic circumstances, the obtained parameters (amplitude and phase) would become less informative with the saturation of the response and non-linear analysis would become imperative (Kruggel and von Cramon, 1999; Kruggel et al., 2000). It is likely (although we do not have evidence for this in our data) that the extent of the linear regime may be different for different brain regions, and thus this might affect the spatial invariance of our analysis.

Another limitation of this analysis is the difficulty to identify voxels which may be active in more than one processing stage. Since the phase measurement is essentially a center-of-mass estimator, it is highly sensitive to non-local perturbations and thus this method is expected to work only if the contribution of a brain region is confined to a well-defined time interval. Indeed, this limitation should be the general case for linear methods which can be very precise to identify parametrically local deformations (for example a continuous change in delay or duration) but fail for more generic deformations of the response.

Finally, another limitation of our proposed method is that it is based on a slow event-related design. Many paradigms, due to the nature of the task or to the number of conditions, require the use of faster stimulus rates (Dale and Buckner, 1997) and the optimal statistical power has been found to be for an inter-trial spacing close to 5 s (Miezin et al., 2000). Extensions of our strategy to this situation are conceivable, however, and other methods to obtain timing information with a slow TR and a fast ITI have been proposed (Bellgowan et al., 2003; Formisano et al., 2002; Henson et al., 2002)

While our method recovered a plausible ordering of brain activations, examination of the raw phase of the BOLD signal, which is contaminated by the HRF, did not usually reveal a monotonic arrangement with the expected ordering of the stages. Indeed, an intriguing observation was that the BOLD signal in parietal cortex was delayed with respect to the signal in visual or auditory cortices, in contradiction with the sequential order we observed. From our data, we cannot disambiguate between a neuronal and a vascular explanation for this delay. It is possible that task alerting results in a parietal activation, whose onset and duration may have a slower dynamics (either onset or duration) than perceptual processing. This may be the case even if parietal activation is independent of the duration of perceptual processing and thus does not follow it sequentially. Yet two arguments suggest that most likely the observed delay in parietal activity results from non-homogeneities in the hemodynamic response function, probably related to vascular effects. First, the difference in the phase we observed exceeds 500 ms, far longer than any neuronal delay plausibly associated with a late onset of parietal activity. For instance, single cell studies in behaving monkeys performing a decision task have find an onset of activation in parietal cortex with a relatively fixed delay of about 200 ms (Mazurek et al., 2003; Roitman and Shadlen, 2002). Second, the variability of the raw phase was very high, even within neighboring voxels of the same cortical region. The variability observed here is comparable to what has been found previously (Lee et al., 1995; Saad et al., 2001): HRFs in the vicinity of large blood vessels can show latencies up to 2.5 s longer than those from the parenchyma. This finding highlights the importance of a relative measure of latency, factoring out the effects of the HRF. Such a differential approach is essential for cross-region comparisons but also for analysis of neighboring voxels within the same region.

While this present work does not attempt to be meta-methodological comparison in the area of fMRI timing estimates, it is important to discuss the comparative advantages and disadvantages of our proposed method with the classic general linear model (GLS) using the HRF as basis functions. In principle, theory predicts that if the model of the HRF is correct, the GLM should be more efficient than our regression to sine and cosine functions. In practice, however, these functions provide fairly accurate approximations of the HRF implying that one can use these basis functions without a significant loss in power. Moreover, methods based on a precise shape of the HRF and its derivative are more sensitive to the particular goodness of this fit and thus become problematic when attempting to compare results across different voxels due to the high HRF variability. In addition, for the GLM one would need to know the duration of each stage, unless different durations are modeled simultaneously. Indeed, in the GLM, one could potentially design a model which includes all the processes involved in a particular trial. If this would work, it would overcome a major limitation of our proposed model; the inability to detect a voxel involved in multiple stages. Unfortunately such a design matrix would be very highly correlated and likely to become singular and thus in practice this approach becomes very difficult. On the other hand, the advantage of our proposed model is that it poses a natural decomposition (which can be found in a single model) to detect simultaneously the duration and delay of the activations of each voxel.

Our present effort continues a series of methodological and cognitive efforts devoted to parse the sequence of activations in a cognitive task using fMRI see (Formisano and Goebel, 2003; Menon and Kim, 1999) for reviews and to the integration of fMRI and MEG (Dale et al., 2000). Using a field of view restricted to regions of interest (ROI) and scanning only a few slices, thus allowing considerably faster sampling rates, latency differences were measured in a variety of tasks which include sensory and sensory-motor (Menon et al., 1998; Weilke et al., 2001), motor sequences (Kim et al., 1997; Richter et al., 1997a,b; Weilke et al., 2001) and mental rotation (Richter et al., 1997a,b; 2000). Latency measurements have also been obtained in whole-brain studies in a

variety of cognitive tasks (Formisano et al., 2002; Henson et al., 2002; Lee et al., 2005; Schacter et al., 1997; Thierry et al., 1999; Wildgruber et al., 1999). In Formisano et al. (2002), for particular ROI, the width and the onset delay of the modeled hemodynamic response function (HRF) were estimated and regions were parceled according to whether their delay or they width covaried with RT. In these different studies, a variety of methods have been used to measure timing parameters from the BOLD signal (see Formisano and Goebel, 2003 for a review) indicating that fine temporal fMRI measurements, within the psychological time scale, while not necessarily easy to achieve, are feasible and reliable. Bellgowan et al. (2003) pushed this analysis further showing that a methodological effort, combined with appropriate task comparisons, can produce difference maps that standardize the delay, and width measures between voxels. The present experiment used a slow and complex cognitive task. Its main purpose was to keep the duration and onset of all the stages under direct experimental control. While this choice was made for methodological validation purposes, future experiments should assess whether the present method can recover the activation sequence in tasks where the brain activation sequences and durations are unknown (although a cognitive model may be available). In principle, our analysis (or similar variants) should be appropriate to address numerous timing questions in neuroscience. For example covariations of the BOLD signal phase with response time could be studied in order to identify invariant regions which do not vary with RT, regions whose durations covaries with RT (sources of the response decision process), and regions whose delay varies with RT (stages following response decision; see Sigman and Dehaene, 2005). Our approach provides a natural extension of Sternberg's additive-factors method, which involves measuring the impact of experimental manipulations on chronometric measures in order to evaluate the sequential organization of brain processes (Sternberg, 1969, 2004). The present method generalizes easily to a factorial design to examine when, and in which brain areas, two different experimental factors impact on brain activation measures. Such a factorial design was applied previously with a different analytic approach to obtain onset and duration changes invariant relative to the HRF (Bellgowan et al., 2003). Combined with a precise psychological model of the chronometry of the task, factorial designs could lead to a complete parsing of any cognitive task. Indeed, our method is capable of going beyond classical additive-factor analysis by revealing brain regions active before, during or after the process manipulated by a given experimental factor. As a final example, this type of analysis seems very adequate to address the latencies in cognitive processing which reflect mental bottlenecks in dual-task performance (Pashler, 1984; Sigman and Dehaene, 2005, 2006). Imaging results demonstrate that dual-task delays need not be associated with any substantial change in the amplitude of BOLD activation (Jiang et al., 2004). In such a situation, a sequential analysis of brain activations may be the only way to understand the cerebral origins of the dual-task bottleneck.

Acknowledgments

We thank Ghislaine Dehaene-Lambertz for substantial experimental help. MS is supported by a Human Frontiers Science Program Fellowship and SD by a centennial fellowship of the McDonnell Foundation.

References

Aguirre, G.K., Zarahn, E., D'Esposito, M., 1998. The variability of human, BOLD hemodynamic responses. NeuroImage 8, 360–369.

Andersen, R.A., 1995. Encoding of intention and spatial location in the posterior parietal cortex. Cereb. Cortex 5, 457–469.

Bellgowan, P.S., Saad, Z.S., Bandettini, P.A., 2003. Understanding neural system dynamics through task modulation and measurement of functional MRI amplitude, latency, and width. Proc. Natl. Acad. Sci. U. S. A. 100, 1415–1419.

Binder, J.R., Frost, J.A., Hammeke, T.A., Bellgowan, P.S., Springer, J.A., Kaufman, J.N., Possing, E.T., 2000. Human temporal lobe activation by speech and nonspeech sounds. Cereb. Cortex 10, 512–528.

Boynton, G.M., Engel, S.A., Glover, G.H., Heeger, D.J., 1996. Linear systems analysis of functional magnetic resonance imaging in human V1. J. Neurosci. 16, 4207–4221.

Buckner, R.L., 2003. The hemodynamic inverse problem: making inferences about neural activity from measured MRI signals. Proc. Natl. Acad. Sci. U. S. A. 100, 2177–2179.

Buckner, R.L., Bandettini, P.A., O'Craven, K.M., Savoy, R.L., Petersen, S.E., Raichle, M.E., Rosen, B.R., 1996. Detection of cortical activation during averaged single trials of a cognitive task using functional magnetic resonance imaging. Proc. Natl. Acad. Sci. U. S. A. 93, 14878–14883.

Cohen, L., Dehaene, S., 2004. Specialization within the ventral stream: the case for the visual word form area. NeuroImage 22, 466–476.

Colby, C.L., Duhamel, J.R., Goldberg, M.E., 1996. Visual, presaccadic, and cognitive activation of single neurons in monkey lateral intraparietal area. J. Neurophysiol. 76, 2841–2852.

Dale, A.M., Buckner, R.L., 1997. Selective averaging of rapidly presented trials using fMRI. Hum. Brain Mapp. 5, 329–340.

Dale, A.M., Liu, A.K., Fischl, B.R., Buckner, R.L., Belliveau, J.W., Lewine, J.D., Halgren, E., 2000. Dynamic statistical parametric mapping: combining fMRI and MEG for high-resolution imaging of cortical activity. Neuron 26, 55–67.

Dehaene, S., Spelke, E., Pinel, P., Stanescu, R., Tsivkin, S., 1999. Sources of mathematical thinking: behavioral and brain-imaging evidence. Science 284, 970–974.

Doyon, J., Owen, A.M., Petrides, M., Sziklas, V., Evans, A.C., 1996. Functional anatomy of visuomotor skill learning in human subjects examined with positron emission tomography. Eur. J. Neurosci. 8, 637–648.

Eger, E., Sterzer, P., Russ, M.O., Giraud, A.L., Kleinschmidt, A., 2003. A supramodal number representation in human intraparietal cortex. Neuron 37, 719–725.

Formisano, E., Goebel, R., 2003. Tracking cognitive processes with functional MRI mental chronometry. Curr. Opin. Neurobiol. 13, 174–181.

Formisano, E., Linden, D.E., Di Salle, F., Trojano, L., Esposito, F., Sack, A.T., Grossi, D., Zanella, F.E., Goebel, R., 2002. Tracking the mind's image in the brain: I. Time-resolved fMRI during visuospatial mental imagery. Neuron 35, 185–194.

Fries, W., Swihart, A.A., 1990. Disturbance of rhythm sense following right hemisphere damage. Neuropsychologia 28, 1317–1323.

Frot, M., Mauguiere, F., 1999. Timing and spatial distribution of somatosensory responses recorded in the upper bank of the sylvian fissure (SII area) in humans. Cereb. Cortex 9, 854–863.

Graybiel, A.M., Kimura, M., 1995. Adaptative neural networks in the basal ganglia. In: Houk, J.C., Davis, J.L., Beiser, D.G. (Eds.), Models of Information Processing in the Basal Ganglia. MIT Press, Cambridge, pp. 103–116.

Gusnard, D.A., Raichle, M.E., 2001. Searching for a baseline: functional imaging and the resting human brain. Nat. Rev., Neurosci. 2, 685–694.

Henson, R., Shallice, T., Dolan, R., 2000. Neuroimaging evidence for dissociable forms of repetition priming. Science 287, 1269–1272.

Henson, R.N., Price, C.J., Rugg, M.D., Turner, R., Friston, K.J., 2002. Detecting latency differences in event-related BOLD responses: application to words versus nonwords and initial versus repeated face presentations. NeuroImage 15, 83–97.

Jiang, Y., Saxe, R., Kanwisher, N., 2004. Functional magnetic resonance imaging provides new constraints on Theories of the Psychological Refractory Period. Psychol. Sci. 15 (6), 390–396.

Kim, S.G., Richter, W., Ugurbil, K., 1997. Limitations of temporal resolution in functional MRI. Magn. Reson. Med. 37, 631–636.

Koechlin, E., Danek, A., Burnod, Y., Grafman, J., 2002. Medial prefrontal and subcortical mechanisms underlying the acquisition of motor and cognitive action sequences in humans. Neuron 35, 371–381.

Kruggel, F., von Cramon, D.Y., 1999. Temporal properties of the hemodynamic response in functional MRI. Hum. Brain Mapp. 8, 259–271.

Kruggel, F., Zysset, S., von Cramon, D.Y., 2000. Nonlinear regression of functional MRI data: an item recognition task study. NeuroImage 12, 173–183.

Lange, N., Zeger, S.L., 1997. Non-linear Fourier time series analysis for human brain mapping by functional magnetic resonance imaging (with Discussion). Appl. Stat. 46, 1–29.

Lee, A.T., Glover, G.H., Meyer, C.H., 1995. Discrimination of large venous vessels in time-course spiral blood-oxygen-level-dependent magnetic-resonance functional neuroimaging. Magn. Reson. Med. 33, 745–754.

Lee, S.H., Blake, R., Heeger, D.J., 2005. Traveling waves of activity in primary visual cortex during binocular rivalry. Nat. Neurosci. 8, 22–23.

Liao, C.H., Worsley, K.J., Poline, J.B., Aston, J.A., Duncan, G.H., Evans, A.C., 2002. Estimating the delay of the fMRI response. NeuroImage 16, 593–606.

Mazurek, M.E., Roitman, J.D., Ditterich, J., Shadlen, M.N., 2003. A role for neural integrators in perceptual decision making. Cereb. Cortex 13, 1257–1269.

Menon, R.S., Kim, S.G., 1999. Spatial and temporal limits in cognitive neuroimaging with fMRI. Trends Cogn. Sci. 3, 207–216.

Menon, R.S., Luknowsky, D.C., Gati, J.S., 1998. Mental chronometry using latency-resolved functional MRI. Proc. Natl. Acad. Sci. U. S. A. 95, 10902–10907.

Miezin, F.M., Maccotta, L., Ollinger, J.M., Petersen, S.E., Buckner, R.L., 2000. Characterizing the hemodynamic response: effects of presentation rate, sampling procedure, and the possibility of ordering brain activity based on relative timing. NeuroImage 11, 735–759.

Pashler, H., 1984. Processing stages in overlapping tasks: evidence for a central bottleneck. J. Exp. Psychol. Hum. Percept. Perform 10, 358–377.

Posner, M.I., 1978. Chronmetric Explorations of Mind. Erlbaum, Hilsdale, NJ.

Purdon, P.L., Solo, V., Weisskoff, R.M., Brown, E.N., 2001. Locally regularized spatiotemporal modeling and model comparison for functional MRI. NeuroImage 14, 912–923.

Rajapakse, J.C., Kruggel, F., Maisog, J.M., von Cramon, D.Y., 1998. Modeling hemodynamic response for analysis of functional MRI time-series. Hum. Brain Mapp. 6, 283–300.

Richter, W., Andersen, P.M., Georgopoulos, A.P., Kim, S.G., 1997a. Sequential activity in human motor areas during a delayed cued finger movement task studied by time-resolved fMRI. NeuroReport 8, 1257–1261.

Richter, W., Ugurbil, K., Georgopoulos, A., Kim, S.G., 1997b. Time-resolved fMRI of mental rotation. NeuroReport 8, 3697–3702.

Richter, W., Somorjai, R., Summers, R., Jarmasz, M., Menon, R.S., Gati, J.S., Georgopoulos, A.P., Tegeler, C., Ugurbil, K., Kim, S.G., 2000. Motor area activity during mental rotation studied by time-resolved single-trial fMRI. J. Cogn. Neurosci. 12, 310–320.

Riecker, A., Wildgruber, D., Dogil, G., Grodd, W., Ackermann, H., 2002. Hemispheric lateralization effects of rhythm implementation during syllable repetitions: an fMRI study. NeuroImage 16, 169–176.

Robbins, T.W., Everitt, B.J., 1996. Neurobehavioural mechanisms of reward and motivation. Curr. Opin. Neurobiol. 6, 228–236.

Roitman, J.D., Shadlen, M.N., 2002. Response of neurons in the lateral intraparietal area during a combined visual discrimination reaction time task. J. Neurosci. 22, 9475–9489.

Rosen, B.R., Buckner, R.L., Dale, A.M., 1998. Event-related functional MRI: past, present, and future. Proc. Natl. Acad. Sci. U. S. A. 95, 773–780.

Saad, Z.S., Ropella, K.M., Cox, R.W., DeYoe, E.A., 2001. Analysis and use of FMRI response delays. Hum. Brain Mapp. 13, 74–93.

Saad, Z.S., DeYoe, E.A., Ropella, K.M., 2003. Estimation of FMRI response delays. NeuroImage 18, 494–504.

Schacter, D.L., Buckner, R.L., Koutstaal, W., Dale, A.M., Rosen, B.R., 1997. Late onset of anterior prefrontal activity during true and false recognition: an event-related fMRI study. NeuroImage 6, 259–269.

Schultz, W., Apicella, P., Romo, R., Scarnati, E., 1995. Context-dependent activity in primate striatum reflecting past and future behavioral events. In: Houk, J.C., Davis, J.L., Beiser, D.G. (Eds.), Models of Information Processing in the Basal Ganglia. MIT Press, Cambridge, pp. 11–26.

Scott, S.K., Johnsrude, I.S., 2003. The neuroanatomical and functional organization of speech perception. Trends Neurosci. 26, 100–107.

Sigman, M., Dehaene, S., 2005. Parsing a cognitive task: a characterization of the mind's bottleneck. PLoS Biol. 3, e37.

Sigman, M., Dehaene, S., 2006. Dynamics of the central bottleneck: dual-task and task uncertainty. PLoS Biol. 4, e220.

Sternberg, S., 1969. The discovery of processing stages: extension of Donders' method. In: Koster, W.G. (Ed.), Attention and Performance II. North-Holland Publishing, Amsterdam, pp. 276–315.

Sternberg, S., 2004. Separate modifiability and the search for processing modules. In: Kanwisher, N., Duncan, J. (Eds.), Attention and Performance XX. Oxford Univ. Press, Oxford.

Thierry, G., Boulanouar, K., Kherif, F., Ranjeva, J.P., Demonet, J.F., 1999. Temporal sorting of neural components underlying phonological processing. NeuroReport 10, 2599–2603.

Weilke, F., Spiegel, S., Boecker, H., von Einsiedel, H.G., Conrad, B., Schwaiger, M., Erhard, P., 2001. Time-resolved fMRI of activation patterns in M1 and SMA during complex voluntary movement. J. Neurophysiol. 85, 1858–1863.

Wildgruber, D., Kischka, U., Ackermann, H., Klose, U., Grodd, W., 1999. Dynamic pattern of brain activation during sequencing of word strings evaluated by fMRI. Brain Res. Cogn. Brain Res. 7, 285–294.